

CHAOTICITY ANALYSIS OF THE CURRENT THROUGH PURE,
HYDROGENATED AND HYDROPHOBICALLY MODIFIED PEG-SI THIN
FILMS UNDER VARYING RELATIVE HUMIDITY

by

Kaan Atak

B.S., Physics, Boğaziçi University, 2000

M.S., Physics, Boğaziçi University, 2003

Submitted to the Institute for Graduate Studies in
Science and Engineering in partial fulfillment of
the requirements for the degree of
Doctor of Philosophy

Graduate Program in Physics

Boğaziçi University

2009

DATE OF APPROVAL: 20.May.2009

ACKNOWLEDGEMENTS

In my M.S. Thesis, I wrote, “It was a long journey”. Now I should say that, this second journey was much longer.

I had guides... Prof. Avadis Hacınlıyan shared his limitless intelligence, energy, love. Prof. Yani Skarlatos shared his joy of life as before. Prof. Gülen Aktaş was there in the difficult moments. Assist. Prof. Gökhan Şahin was my old friend, he evolved to be my teacher. Prof. Haluk Beker gave his precious help at the final moments. Prof. Naci İnci provided critical advice.

I had companions... Orhan Özgür Aybar was my teammate, we walked the same road. His motivation boosted mine. Assist. Prof. Özgül Kurtuluş, my old companion, shared her work with me.

As the journey was long, the gains were big as well as the losses. I miss Ali Ayan, my beloved friend, his memory will be with us, as we continue to breathe.

ABSTRACT

CHAOTICITY ANALYSIS OF THE CURRENT THROUGH PURE, HYDROGENATED AND HYDROPHOBICALLY MODIFIED PEG-SI THIN FILMS UNDER VARYING RELATIVE HUMIDITY

Polyethylene Glycol is known to have an irregular current characteristic under constant voltage and slowly varying relative humidity. In this study the current through a thin film of Gamma-isocyanatopropyltriethoxysilane added polyethylene glycol (PEG-Si), its hydrogenated, and hydrophobically modified forms is measured as a function of increasing relative humidity at equal time steps and analyzed for chaoticity. In previous studies it has been suggested that, after reaching a certain relative humidity level, a phase transition occurs from a semi crystalline state to a gel state. We propose that the irregular behavior of current through PEG-Si thin films as a function of increasing relative humidity could best be analyzed for chaoticity using both time series analysis and detrended fluctuation analysis; the relative humidity is kept as a slowly varying parameter. The presence of more than one regime is suggested by the calculation of the maximal Lyapunov exponents. Furthermore, the maximal Lyapunov exponent in each of the regimes was positive, thus confirming the presence of low dimensional chaos. The regime change signaled by the changing values of the maximal Lyapunov exponent occurs around a relative humidity of 70% consistent with the phase transition from semi crystalline state to gel state. Detrended fluctuation analysis has also been performed; this also confirms the presence of at least two different regimes, in agreement with the behavior of the maximal Lyapunov exponent in the time series analysis. Our study also confirms that the improvement in stability of the current through PEG-Si can be performed by hydrogenating and hydrophobically modifying PEG-Si.

ÖZET

DEĞİŞEN BAĞIL NEM ALTINDA SAF, HİDROJENE VE HİDROFOBİK OLARAK DEĞİŞTİRİLMİŞ PEG-Sİ İNCE FİMLERDEN GEÇEN AKIMIN KAOS ANALİZİ

Polietilen Glikol'ün sabit voltaj ve yavaş değişen bağıl nem altında düzensiz bir akım karakteristiği olduğu bilinmektedir. Bu çalışmada, ince film halindeki, Gama-izosyanatopropiltrioksolan eklenmiş polietilen glikolden ve onun hidrojene edilmiş ve hidrofobik olarak modifiye edilmiş formlarından geçen akım, artan bağıl nemin bir fonksiyonu olarak, eşit zaman aralıklarında kaos için analiz edilmiştir. Geçmiş çalışmalarda belli bir bağıl nem seviyesine ulaşınca yarı kristal halden jel haline faz geçişi olduğu önerilmiştir. PEG-Si ince filminden artan bağıl nemin bir fonksiyonu olarak geçen akımdaki düzensiz davranışın, kaos bağlamında, bağıl nem yavaş değişen bir parametre halinde tutularak, zaman serisi analizi ve eğilimsizleştirilmiş dalgalanma analizi kullanılarak analiz edilebileceğini öneriyoruz. Maksimal Lyapunov üstelleri hesabıyla, birden fazla rejimin varlığı önerilmektedir. Ayrıca, her rejimdeki maksimal Lyapunov üsteli pozitif çıkmakta, bu da düşük boyutlu kaosu varlığını teyit etmektedir. Maksimal Lyapunov üstellerinin değerlerinin değişmesinin işaret ettiği rejim değişikliği %70'lik bağıl nem değeri civarında vuku bulmaktadır ve yarı kristal halden jel hale geçiş ile uyum içerisindedir. Eğilimsizleştirilmiş dalgalanma analizi yapılmış, zaman serisi analizindeki maksimal Lyapunov üstellerinin davranışı ile uzlaşma içerisinde, en az iki farklı rejimin varlığı teyit edilmiştir. Bunlara ilaveten, çalışmamızla, PEG-Si'den geçen akımın stabilitesindeki iyileşmenin PEG-Si'yi hidrojene ederek ve hidrofobik olarak modifiye ederek sağlanabileceği teyit edilmiştir.

TABLE OF CONTENTS

ACKNOWLEDGEMENTS	iv
ABSTRACT	v
ÖZET	vi
LIST OF FIGURES	viii
LIST OF TABLES	x
LIST OF SYMBOLS/ABBREVIATIONS	xi
1. INTRODUCTION	1
2. POLYMERS	3
2.1. Polyethylene Glycol	3
2.2. Hydrogenated Polyethylene Glycol	4
2.3. Hydrophobically Modified Polyethylene Glycol	6
3. NONLINEAR TIME SERIES ANALYSIS	9
3.1. Reconstruction of Phase Space	10
3.2. Lyapunov Exponents	13
4. DETRENDED FLUCTUATION ANALYSIS	20
5. CONCLUSIONS	24
APPENDIX A: Lorenz Equations	26
REFERENCES	28

LIST OF FIGURES

Figure 2.1.	Chemical structure of polyethylene glycol	4
Figure 2.2.	Current vs. Time of PEG-Si	5
Figure 2.3.	Current vs. Relative Humidity of PEG-Si	5
Figure 2.4.	Current vs. Time of hydrogenated PEG-Si	6
Figure 2.5.	Current vs. Relative Humidity of hydrogenated PEG-Si	7
Figure 2.6.	Current vs. Time of hydrophobically modified PEG-Si	7
Figure 2.7.	Current vs. Relative Humidity of hydrophobically modified PEG-Si	8
Figure 3.1.	A typical average mutual information vs. delay time graph	12
Figure 3.2.	A typical percentage of false nearest neighbors vs. embedding dimension graph	14
Figure 3.3.	Logarithm of the Stretching Factor vs. Iteration	16
Figure 3.4.	Maximal Lyapunov Exponent vs. Relative Humidity of PEG-Si	16
Figure 3.5.	Maximal Lyapunov Exponent vs. Relative Humidity of hydrophobically modified PEG-Si	17
Figure 3.6.	Maximal Lyapunov Exponent vs. Relative Humidity of hydrogenated PEG-Si	18

Figure 3.7.	Relative Humidity vs. Time of PEG-Si.	19
Figure 3.8.	Stretched exponential relaxation function fit of the time dependence of Relative Humidity, $RH = a_1(1 - a_2 \exp(-(t/\tau)^\alpha))$ with $a_1 = 75.7259 \pm 0.002161$, $a_2 = 0.699292 \pm 0.0001653$, $\tau = 41041 \pm 15.78$ and $\alpha = 0.686974 \pm 0.0002406$	19
Figure 4.1.	Average fluctuation vs. box size for the PEG-Si sample	22
Figure 4.2.	Average fluctuation vs. box size for the hydrophobically modified PEG-Si sample	22
Figure 4.3.	Average fluctuation vs. box size for the hydrogenated PEG-Si sample	23
Figure A.1.	Lorenz Attractor	27
Figure A.2.	Time evolution of the first component of the Lorenz Attractor . . .	27

LIST OF TABLES

Table 4.1.	The correlations implied by the corresponding DFA exponents . . .	21
Table 4.2.	DFA exponents	21

LIST OF SYMBOLS/ABBREVIATIONS

a	Fit parameter
a_i	i 'th measurement from system A
b_j	j 'th measurement from system B
d	Embedding dimension
I	Current
J	Jacobian matrix
N	Number of measurements
R	Distance between nearest neighbor points
RH	Relative humidity
$P_A(a)$	Probability of measuring a in system A
$P_{AB}(a, b)$	Joint probability of measuring a and b in systems A and B
$S(\tau)$	Average mutual information function
$\vec{y}(t)$	Reconstructed vector
α	DFA exponent
δr	Separation between two trajectories in phase space
λ	Lyapunov exponent
ρ	Rayleigh number
σ	Prandtl number
τ	Delay time
D.C.	Direct Current
DFA	Detrended Fluctuation Analysis
PAF	Perfluoroalkyl alcohol
PAF-Si	Gamma-isocyanatopropyltriethoxysilane added Perfluoroalkyl alcohol
PEG	Polyethylene glycol
PEG-Si	Gamma-isocyanatopropyltriethoxysilane added Polyethylene glycol

PET	Polyethylene terephthalate
PVC	Polyvinyl chloride
TISEAN	A nonlinear time series analysis software

1. INTRODUCTION

Hydrophilic polymers attract attention because of their absorption, desorption and swelling behavior under exposure to water vapor and certain chemicals. Depending on environmental conditions (temperature, humidity, the structure of the polymer etc.) diffusion of the penetrants in the polymer networks shows different dynamical properties. If water molecules penetrate a polymer sample, the macromolecular chains rearrange themselves towards new conformations. The nature of the transport process and the electrical, optical and physical properties of the polymer are determined by the diffusion rate of the penetrant's molecules and the relaxation processes [29].

Polyethylene glycol (PEG) is one of the most examined hydrophilic polymers, that has properties sensitive to the changes in relative humidity and the chemicals used as substrates. It is known that PEG has a problem of stability; if exposed to water vapor, it swells and dissolves easily at high humidity levels. The instability of the structure and the transport properties in the long term constitute a general problem of polymer films produced by the physisorption of polymer molecules to the substrate material.

In this study, the irregular current characteristic under constant voltage and slowly varying humidity, through a thin film of Gamma-isocyanatopropyltriethoxysilane added Polyethylene glycol (PEG-Si), as a function of increasing relative humidity, at equal time steps is analyzed for chaoticity. In a previous study [4], it has been suggested that, after reaching a certain relative humidity level, a phase transition occurs from a semi crystalline state to a gel state, and the resulting fluctuations in the elastic force relaxations and in the number of hydrogen bonds cause the irregularities in the current. We suggest that, the irregular behavior of current through these films as a function of increasing relative humidity could be analyzed for chaoticity, where the relative humidity is kept as a slowly varying parameter and the data is split into approximately 2.5% time bins. The results also indicate that the above mentioned phase transition is signalled by the sudden change in the maximal Lyapunov exponent with changing relative humidity.

In the aforementioned study, in order to alleviate the instability problem in the current behaviour of PEG-Si, two different modifications have been applied. The first method was to hydrogenate PEG, and the second method was to hydrophobically modify it. To some extent, the modifications were able to cure the stability problem. In our study, in addition to the analysis on PEG-Si, we repeated the analysis on hydrogenated and hydrophobically modified PEG-Si samples and investigated the possible effects of the modifications.

The outline of the thesis is as follows. In the first chapter, I briefly introduce polymers, describe pure, hydrogenated and hydrophobically modified PEG-Si, give details about the preparation of the samples and the experimental setup and present the obtained data.

In the second chapter, I briefly introduce chaos, and give a detailed description of the nonlinear time series analysis, present the application of nonlinear time series analysis to the current time series of pure, hydrogenated and hydrophobically modified PEG-Si, and give the results.

In the third chapter I give a description of the detrended fluctuation analysis, present the application of the detrended fluctuation analysis to the data at hand and give the results.

In the last chapter I present the results and conclude the thesis.

2. POLYMERS

The word “polymer” is derived from Greek words $\pi\omicron\lambda\upsilon$ (poly) meaning many and $\mu\epsilon\rho\omicron\varsigma$ (meros) meaning part. It is a large molecule (macromolecule) composed of repeating structural units (monomers) connected by chemical bonds. Polymers containing small number of units are called dimers, trimers, tetramers, etc., and the term polymer is reserved for molecules composed of many more units in the order of 10^3 . All the monomers in a polymer need not be identical (for example a copolymer contains more than one type of monomer), and the polymer molecule can be thought of a big network branched in every direction the 3-dimensional bond structure allows [29]. Naturally occurring molecules such as shellac and amber have been used since ancient times but the discovery of the chemical origins had to wait for centuries until Hermann Staudinger’s work in 1922. A variety of naturally occurring biopolymers exist such as cellulose, natural rubber, nucleic acids and the large family of proteins. After Leo Baekeland created the first completely synthetic polymer bakelite in 1907, the door to the synthesis of a virtually infinite family of polymers had opened with PET (polyethylene terephthalate), PVC (polyvinyl chloride) and nylon as everyday examples [3]. The terms crystalline and amorphous in the case of polymers do not apply as two strict structural orientations but rather two extremes of a continuum. Due to the very large complex network structure of most polymers, they cannot be classified as crystalline; rather, we can talk about crystalline regions of this large network. 1-dimensional polymers or polymers with small molecular weight could be conveniently placed in the conventional definition of crystallinity.

2.1. Polyethylene Glycol

Polyethylene glycol (PEG), is a polymer (polyether), which has the chemical structure $HO - CH_2 - (CH_2 - CH_2 - O)_n - CH_2 - OH$ (Fig. 2.1) and molecular formula $C_{2n+2}H_{4n+6}O_{n+2}$. It is prepared by polymerization of ethylene oxide, can have a wide range of molecular weights from 300 g/mol to 10,000,000 g/mol and is soluble in water. It is a very popular molecule and is being used in various fields such as

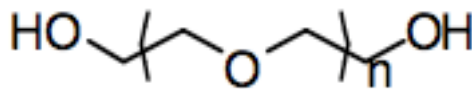


Figure 2.1. Chemical structure of polyethylene glycol

medicine, biochemistry, microbiology, etc.

The data we explore in this study were taken by Erdamar et al. in her PhD studies [4], [24], [29] for the characterization of the conductivity of PEG under varying relative humidity. We took the data from her work and approached the problem using different methods. PEG is water soluble; therefore, it swells when exposed to water vapor and dissolves. This creates a durability problem. A solution to this problem was mixing it by a suitable crosslinking agent, which was in this case, isocyanatopropyltriethoxysilane. For the technical details of sample preparation refer to [29]. The product of this crosslinking process is abbreviated as PEG-Si, which is the main substance under investigation in this study. The resulting substance is coated on glass substrates by either dropping or dip-coating. Afterwards the electrodes were thermally evaporated on the thin film in a coplanar geometry. The samples prepared are inserted in a closed chamber, a D.C. electrical field of $30Vcm^{-1}$ is applied and the resulting current is measured by an electrometer-voltage source (Keithley 6517A). The humidity is changed by placing salt solutions in the chamber. A continuously changing humidity curve is obtained (Fig. 3.7). The following current vs. time (Fig. 2.2) and current vs. relative humidity (Fig. 2.3) characteristics are observed and are shown in the indicated figures [29].

2.2. Hydrogenated Polyethylene Glycol

After obtaining the current characteristics of PEG, it is observed that the current has large time dependent fluctuations in the high humidity region. One of the goals of the original study was to explore the feasibility of building a humidity sensor out of PEG. To stabilize the current, two solutions were proposed. The first one was to

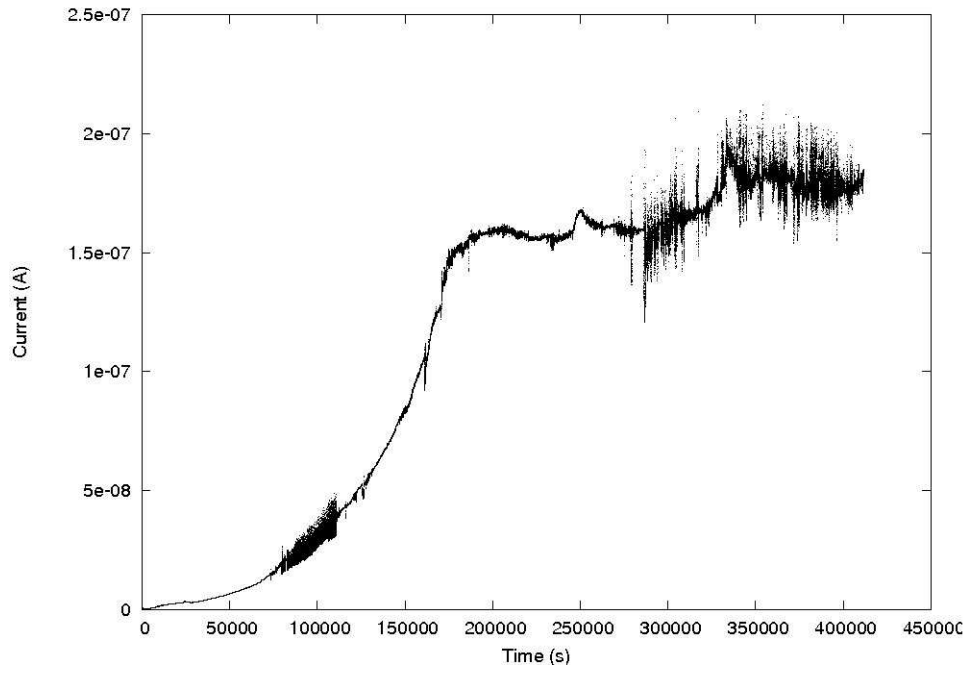


Figure 2.2. Current vs. Time of PEG-Si

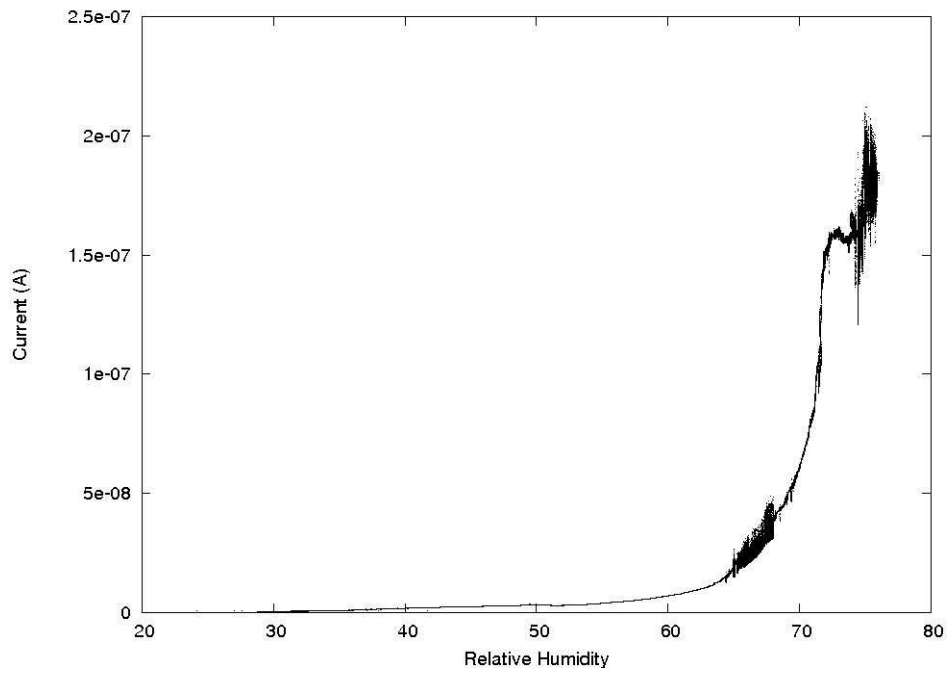


Figure 2.3. Current vs. Relative Humidity of PEG-Si

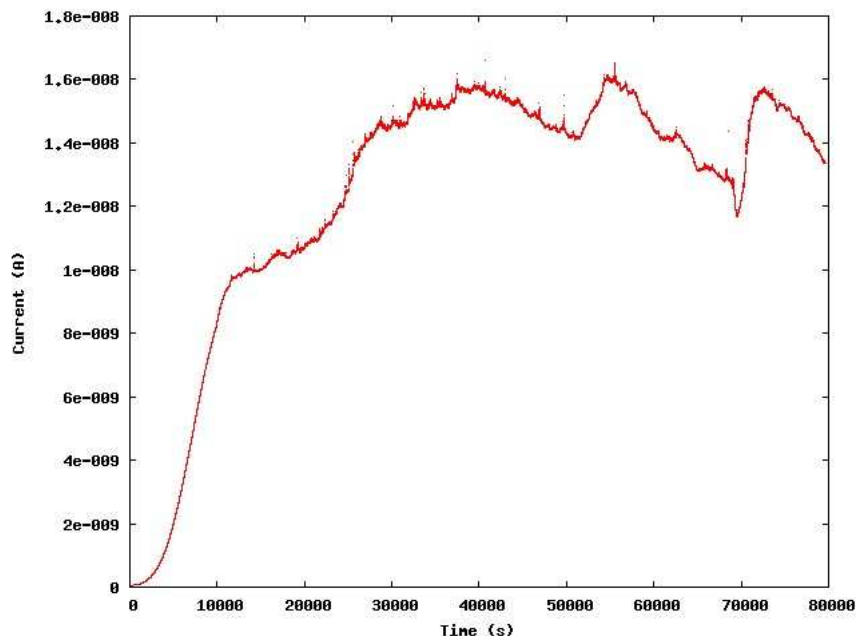


Figure 2.4. Current vs. Time of hydrogenated PEG-Si

hydrogenate PEG by introducing Hydrogen gas to the samples in a vacuum chamber [29]. The current vs. time (Fig. 2.4) and current vs. relative humidity (Fig. 2.5) characteristics are shown.

2.3. Hydrophobically Modified Polyethylene Glycol

The second solution to the instability problem of the current was to hydrophobically modify the samples by mixing PEG with perfluoroalkyl alcohol (PAF), a hydrophobic alcohol. PAF was also crosslinked with isocyanatopropyltriethoxysilane resulting in PAF-Si. The sample under scrutiny is composed of 70% PAF-Si 30% PEG-Si by mass. The current vs. time (Fig. 2.6) and current vs. relative humidity (Fig. 2.7) characteristics are shown.

Of the two proposed methods of current stabilization, hydrophobic modification seems to be the more successful one. At a first glance of the current graphs, it is observed that, the hydrogenated samples possess more fluctuations. In the later chapters this difference will be inspected more closely.

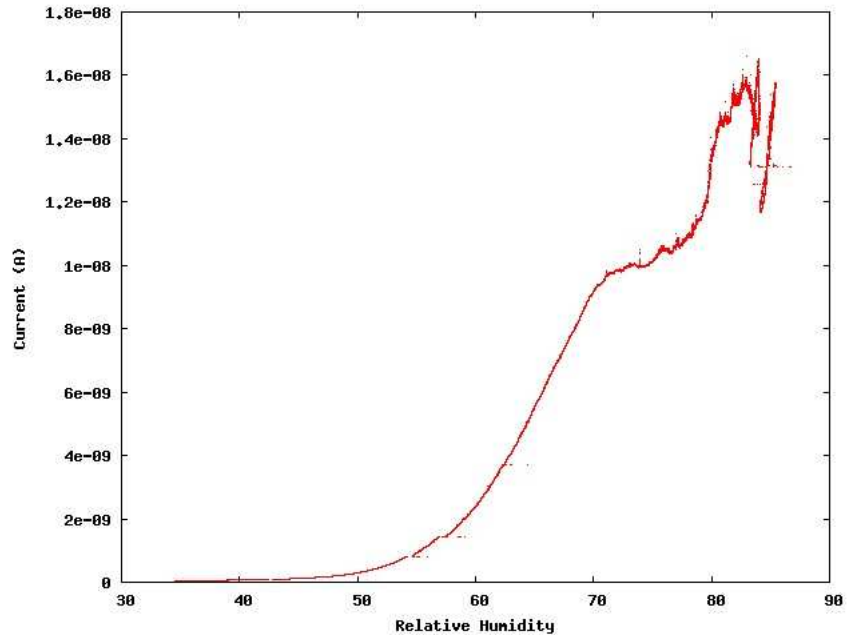


Figure 2.5. Current vs. Relative Humidity of hydrogenated PEG-Si

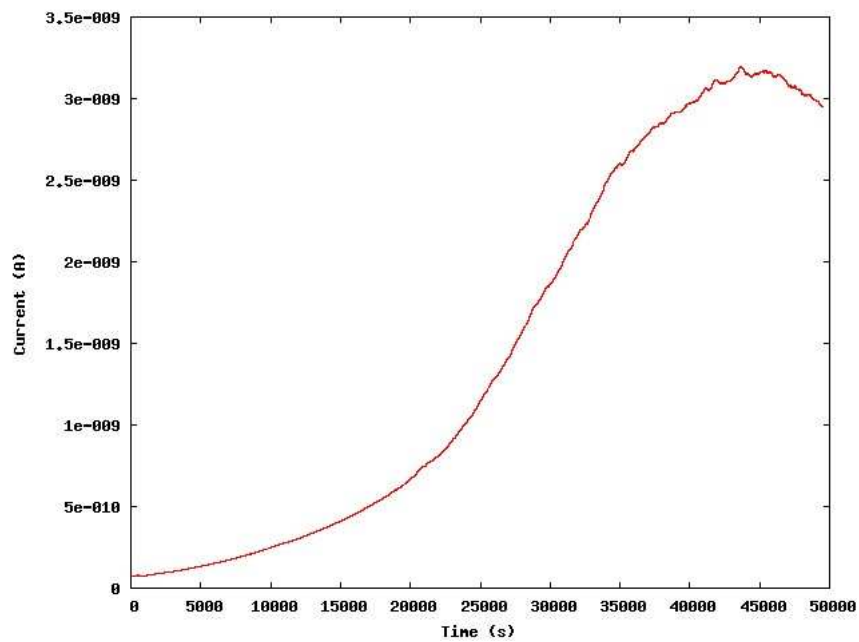


Figure 2.6. Current vs. Time of hydrophobically modified PEG-Si

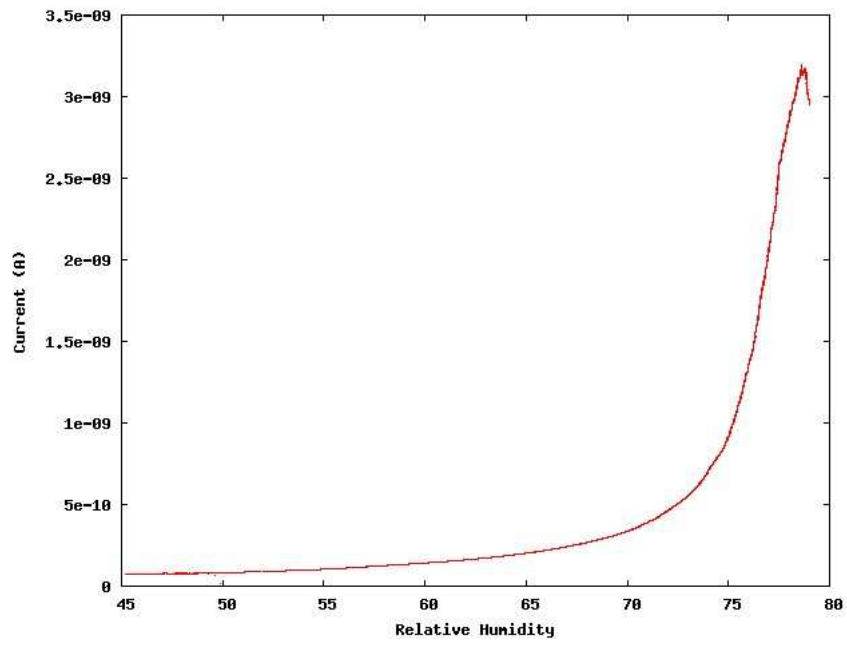


Figure 2.7. Current vs. Relative Humidity of hydrophobically modified PEG-Si

3. NONLINEAR TIME SERIES ANALYSIS

The irregular behaviour of the current through PEG-Si and its derivatives inspired us to apply a nonlinear time series analysis using current as the 1-dimensional sequence. In this chapter a brief description of nonlinear time series analysis and its application to our data will be given.

The word “chaos” is derived from the Ancient Greek word “ $\chi\alpha\omicron\varsigma$ ” meaning “space”, later changed to “disorder”. In mathematical sense it has to be corrected as “unpredictable determinism”. More strictly chaos is aperiodic deterministic behavior with great sensitivity to its initial conditions, popularly known as the “butterfly effect”; a butterfly flapping its wings in İstanbul, may cause a hurricane in Tokyo. Chaos manifests itself in nonlinear systems, linear systems cannot exhibit chaos. The Poincaré-Bendixson theorem asserts that chaos can only arise in a continuous dynamical system ($\frac{d\vec{x}}{dt} = \vec{F}(\vec{x}(t))$) if it has three or more dimensions. However, this restriction does not apply to discrete systems ($\vec{x}(t+1) = \vec{f}(\vec{x}(t))$), which can exhibit chaotic behavior in two or even one dimensional systems. Loosely speaking, if the trajectories in the phase space of a dynamical system confine to a specific subspace, we speak of an attractor in that part of the phase space. The attractor is informally described as a strange attractor if it has non-integer dimension or if the dynamics on it are chaotic. For a detailed treatment of the subject refer to [30]. To be able to extract information from a set of data in the form of a scalar time series from a nonlinear dynamical system, one has to reconstruct the phase space of the system.

To be able to study the effect of relative humidity on the dynamics of electrical conductivity, we divided our data sets, which have in the order of 10^5 points into smaller sets of 10^4 points. In these smaller sets the relative humidity is slowly varying, and each set is represented by its average relative humidity value. The procedures of phase space reconstruction and extraction of Lyapunov exponents are applied to each set. The standard TISEAN software is used for the analyses [34].

3.1. Reconstruction of Phase Space

By performing current measurements at equal time intervals we have at hand a time series of the form $I(t)$ taken from the dynamical system under investigation. From these scalar measurements we have to go to the multidimensional phase space of our dynamical system. The embedding theorem states that, a properly constructed delay embedding space is equivalent to original unobserved phase space [1]. From the scalar current measurements $I(t)$ we have to form vectors of the form;

$$\vec{y}(t) = (I(t), I(t + \tau), \dots, I(t + (d - 1)\tau)) \quad (3.1)$$

in which τ denotes the delay time and d denotes the embedding dimension. The embedding space and dimension need not be exactly the same as the original space and dimension in which the dynamics take place (and most of the time it isn't), however the invariants of the original space are conserved.

The first problem to be handled is to find a proper time delay. Theoretically, if we had an infinite time series, then any time delay would suffice. Naturally one takes it as a multiple of the sampling time (in our case, 1 second). In practice, the time series under investigation are never infinitely long, therefore finding a proper time delay emerges as a problem to be handled. If the time delay chosen is too short, the constructed vectors will be temporally too close and will not be independent enough. If it is too long, the vectors will appear to be random due to chaotic nature of the systems under analysis.

In our study we used the average mutual information function, as the tool to handle the time delay problem. If a_i and b_j are two measurements from the systems A and B , the average mutual information function $S(\tau)$ is defined as;

$$S_{AB} = \sum_{a_i, b_j} P_{AB}(a_i, b_j) \ln \left(\frac{P_{AB}(a_i, b_j)}{P_A(a_i)P_B(b_j)} \right) \quad (3.2)$$

where the probability of observing a out of the set A is $P_A(a)$, the probability of finding b in a measurement of B is $P_B(b)$, and joint probability of the measurement of a and b is $P_{AB}(a, b)$. The part including the natural logarithm function in the above equation is called the mutual information, by summation over all possible measurements one obtains the average mutual information [1].

To apply this definition into the context of our physical system $I(t)$, the set of measurements $I(t)$ becomes the set A , and the measurements after a time lag τ , $I(t + \tau)$ becomes the set B . The average mutual information between observations at t and $t + \tau$, i.e. the average amount of information $I(t + \tau)$ we have, when we make an observation of $I(t)$ is

$$S(\tau) = \sum_t P(I(t), I(t + \tau)) \ln \left(\frac{P(I(t), I(t + \tau))}{P(I(t))P(I(t + \tau))} \right) \quad (3.3)$$

A prescription to find a proper time delay out of the above machinery is to choose the first minimum of $S(\tau)$. This is a rule of thumb rather than a strict rule, most of the time different delay times which have similar values lead to the same dynamical invariants. For a typical average mutual information graph for a set of 10^4 points refer to Fig. 3.1 from which we chose the time delay as 10s.

After choosing a suitable time delay, the choice of the embedding dimension of the reconstructed phase space has to be handled. The embedding theorem tells that if the box counting dimension of the attractor is d_f , then an integer embedding dimension $d_E > 2d_f$ will properly unfold the attractor in the reconstructed phase space. This condition guarantees a proper unfolding, however there are cases where a smaller d_E suffices [1]. Theoretically, any integer dimension greater than the sufficient d_E will also do the job, but in practice both an unnecessarily big dimension costs much greater computational effort, and noise tends to be homogeneous in all dimensions, so effectively one will deal with only noise in these higher dimensions. The method of false nearest neighbors is a useful instrument to give an estimate for the embedding dimension. The method has the following simple logic behind. Beginning with a

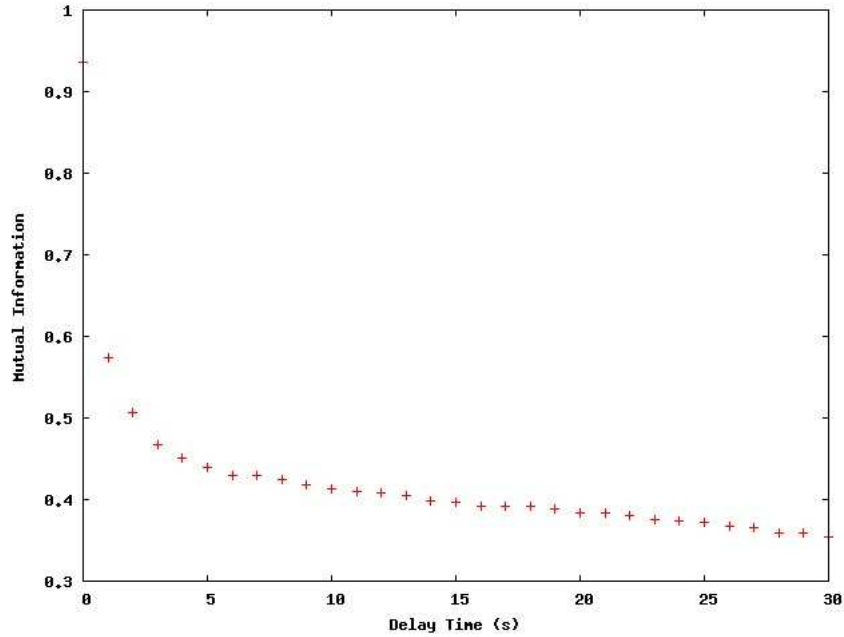


Figure 3.1. A typical average mutual information vs. delay time graph

reconstructed vector with the proper time delay τ and embedding dimension d

$$\vec{y}(t) = (I(t), I(t + \tau), \dots, I(t + (d - 1)\tau)) \quad (3.4)$$

will have a nearest neighbor in the phase space as

$$\vec{y}_{NN}(t) = (I_{NN}(t), I_{NN}(t + \tau), \dots, I_{NN}(t + (d - 1)\tau)) \quad (3.5)$$

If the chosen embedding dimension is not large enough, then the attractor will not unfold properly and due to projection on a lower dimensional space, false data points will fall into each others neighborhood. Increasing the embedding dimension will decrease the number of false neighbors so we have to look for the dimension at which all false neighbors will vanish for each data point, by switching to the next higher dimension. One has to check whether two points in dimension d are still close in dimension $d + 1$. When d is increased to $d + 1$ the extra components of $y(t)$ and $y_{NN}(t)$ will be $I(t + \tau d)$ and $I_{NN}(t + \tau d)$. In order to decide whether $y_{NN}(t)$ is a true neighbor of $y(t)$, one compares the distance between these vectors in d dimensions with the distance between them in $d + 1$ dimensions. If the intervector distances in dimension d and $d + 1$ are

comparable to each other than we have true neighbors. However, if the distance in dimension $d + 1$ is larger than the distance measured in dimension d then $y_{NN}(t)$ is said to be a false one. To formulate this idea, we first have to write the distance between the nearest neighbor points in dimension $d + 1$ as;

$$R_{d+1}^2(t) = \sum_{m=1}^{d+1} \left(I(t + (m-1)\tau) - I_{NN}(t + (m-1)\tau) \right)^2 \quad (3.6)$$

written in terms of the corresponding distance in dimension d as;

$$R_{d+1}^2(t) = R_d^2(t) + \left| I(t + \tau d) - I_{NN}(t + \tau d) \right|^2 \quad (3.7)$$

The following equation will give an idea about the change in the distance as the dimension increases;

$$\left[\frac{R_{d+1}^2(t) - R_d^2(t)}{R_d^2(t)} \right]^{\frac{1}{2}} = \frac{|I(t + \tau d) - I_{NN}(t + \tau d)|}{R_d(t)} \quad (3.8)$$

So one looks for a dimension d for which this ratio will be smaller than a threshold value. For a perfect data this value would be zero, but due to noise and other sources of errors, a reasonable value bigger than zero is chosen. In Fig. 3.2 a typical false nearest neighbor calculation from our system is shown. We chose the embedding dimension as 5 and 6 and did the following calculations accordingly for each dimension with no significant changes in the results.

As we have constructed the phase space, which is equivalent to the original one regarding the dynamical invariants, we will continue with one of the most important dynamical properties, namely, the Lyapunov exponents, and using them arrive to conclusions about the effect of the changing relative humidity to the system we study.

3.2. Lyapunov Exponents

A chaotic dynamical system is very sensitive to its initial conditions, i.e., infinitesimal perturbations of initial conditions will lead to large variations of the orbit in the

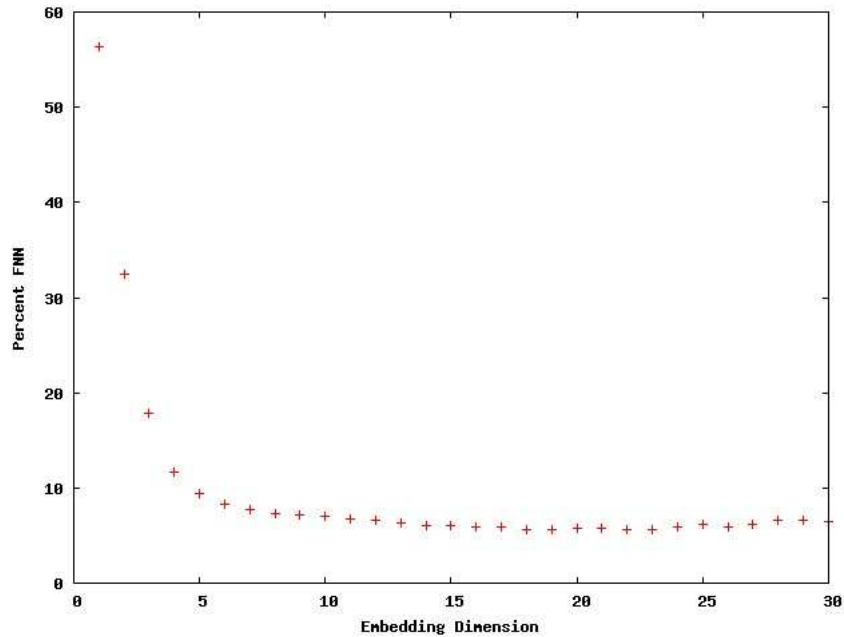


Figure 3.2. A typical percentage of false nearest neighbors vs. embedding dimension graph

phase space. A Lyapunov exponent is a measure of this sensitivity. It is a quantity that characterizes the rate of separation of infinitesimally close trajectories in phase space. Considering two trajectories in phase space with initial separation δr_0 , this separation will diverge as $\delta r(t) = \exp(\lambda t)\delta r_0$ with λ being the Lyapunov exponent. The rate of separation can be different for different orientations of the initial separation vector. So there are d Lyapunov exponents where d is the number of dimensions of the phase space. A chaotic system will have a positive maximal Lyapunov exponent and the others will be negative, creating the stretching and folding effect leading to the geometry of the attractor. Thus a positive maximal Lyapunov exponent, defined as $\lambda = \lim_{t \rightarrow \infty} \frac{1}{t} \ln \frac{\|\delta r(t)\|}{\delta r_0}$, is taken as an indication that the system is chaotic. A more rigorous definition of the Lyapunov spectrum could be given as follows; for a dynamical system with evolution equation f , in a d -dimensional phase space, the spectrum of Lyapunov exponents $\{\lambda_1, \lambda_2, \dots, \lambda_d\}$ in general, depends on the starting point x_0 . The Lyapunov exponents describe the behavior of vectors in the tangent space of the phase space and are defined from the Jacobian matrix $J(x_0) = \frac{df(x)}{dx}$ taken at x_0 . The $J(t)$ matrix describes how a small change at the point x_0 propagates to the final point $f(x_0)$. The matrix $L(x_0)$ is defined as $\lim_{t \rightarrow \infty} (JJ^T)^{\frac{1}{2t}}$. $\Lambda_i(x_0)$ will be the eigenvalues

of $L(x_0)$ and the Lyapunov exponents λ_i will be defined as $\lambda_i(x_0) = \log \Lambda_i(x_0)$. For an ergodic dynamical system, the set of Lyapunov exponents will be the same for almost all starting points.

In our case of finding the maximal Lyapunov exponent of a time series we will use the following algorithm. We start by a point $\vec{y}(t_0)$ in the embedding space with all its neighbors in the vicinity of ϵ . We let the time increase, and look at the growth of the distances between our starting point and these neighbors. If the system at hand is chaotic, these points will expand in space exponentially with time Δt . Therefore we take the logarithm of these distances. We average the results for different t_0 's for the fluctuations to die out.

$$S(\Delta t) = \frac{1}{N} \sum_{t_0=1}^N \ln \left(\frac{1}{|U(\vec{y}(t_0))|} \sum_{\vec{y}(t) \in U(\vec{y}(t_0))} |\vec{y}(t_0 + \Delta t) - \vec{y}(t + \Delta t)| \right) \quad (3.9)$$

The reference points $\vec{y}(t_0)$ are the usual embedding vectors, $U(\vec{y}(t_0))$ is the neighborhood of $\vec{y}(t_0)$ with diameter ϵ . The size of ϵ should be chosen such that it must be as small as possible but large enough to contain at least a few neighbors. If the graph of the stretching factor, $S(\Delta t)$ versus the iteration, Δt results in a robust increase, its slope is assumed to estimate the maximal Lyapunov exponent.

A typical stretching factor versus iteration graph is shown in Fig. 3.3. The straight line indicates the increase in the curve, which is considered as the maximal Lyapunov exponent. This computation is done for all the intervals and in this way the effect of the relative humidity to the maximal Lyapunov exponents is investigated. The results for the pure PEG-Si case are shown in Fig. 3.4. It is understood that, there is a change in the pattern of Lyapunov exponents around the relative humidity value of 70%, and this seems to be consistent with the reported phase transition around this value [29]. In this context we are in the position of proposing a method to track the phase changes, using the Lyapunov exponents in such a dynamical system.

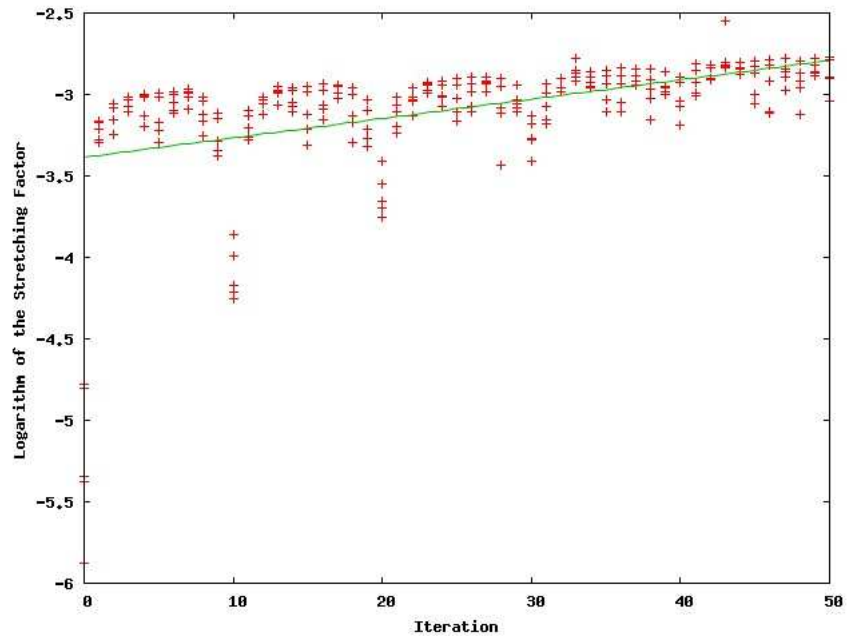


Figure 3.3. Logarithm of the Stretching Factor vs. Iteration

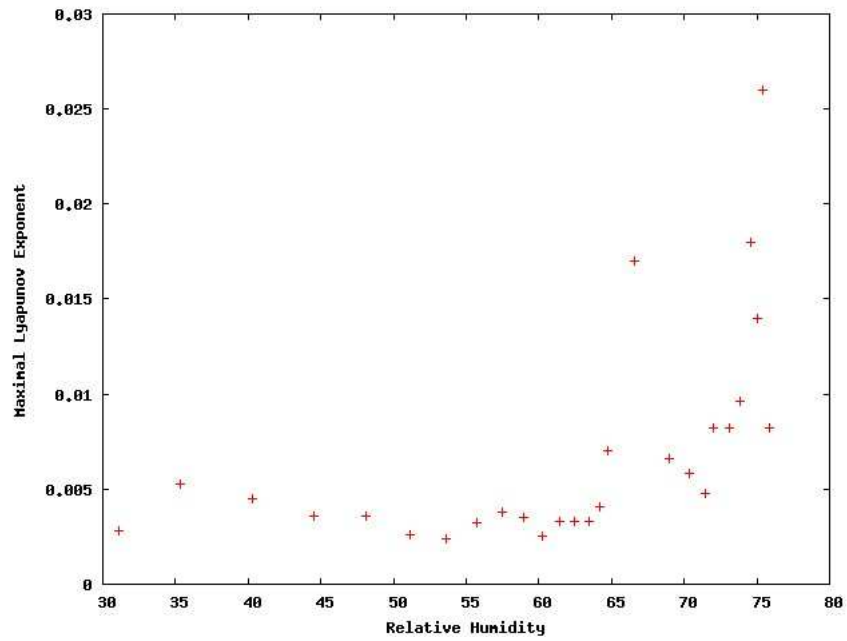


Figure 3.4. Maximal Lyapunov Exponent vs. Relative Humidity of PEG-Si

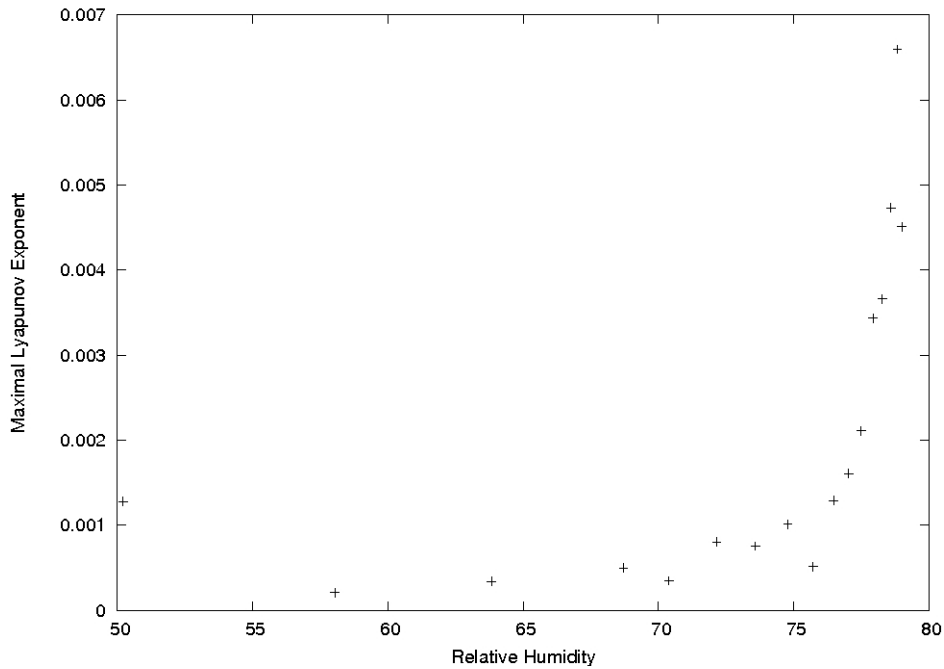


Figure 3.5. Maximal Lyapunov Exponent vs. Relative Humidity of hydrophobically modified PEG-Si

The relative humidity dependence of the maximal Lyapunov exponents for the hydrophobically modified and hydrogenated cases are shown in Fig. 3.5 and Fig. 3.6. The magnitudes of the maximal Lyapunov exponents for these two cases are smaller, this decrease is much more significant particularly for the hydrophobically modified case. The regime change in the maximal Lyapunov exponents is still visible in both cases. These results imply that, the consequences of the efforts of the alleviation of the instabilities in the current could be tracked by nonlinear time series analysis. These efforts, which are more successful for the hydrophobically modified case can be inspected both directly from the current vs. time curves and from the maximal Lyapunov exponents.

Before concluding this chapter we have to mention the possibility that, the chaoticity in the current in our dynamical systems could originate from the relative humidity itself. The relative humidity changing as a function of time is shown in Fig. 3.7. In order to eliminate this possibility, we tried to model this curve using a stretched

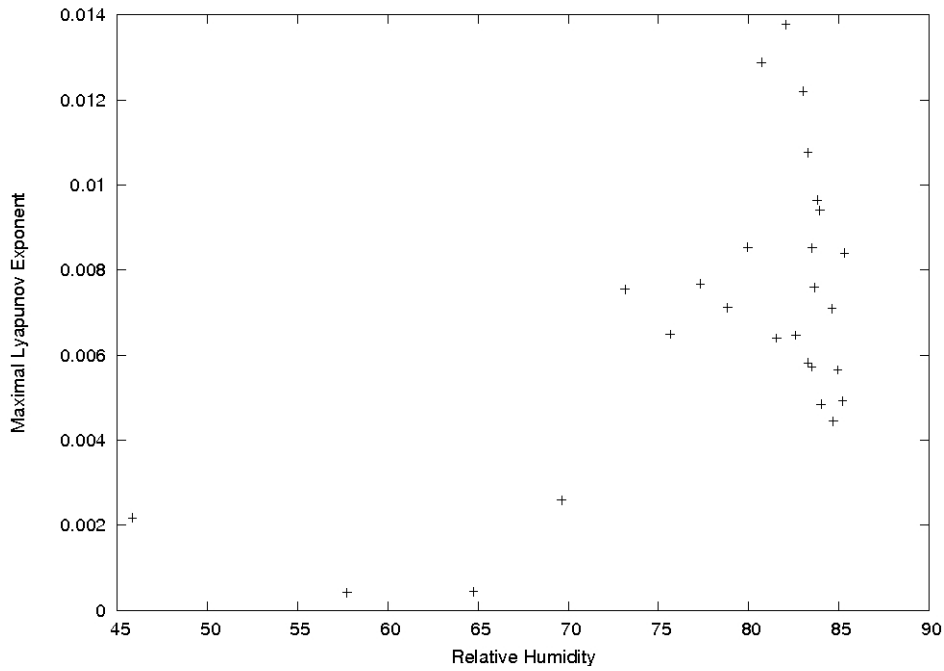


Figure 3.6. Maximal Lyapunov Exponent vs. Relative Humidity of hydrogenated PEG-Si

exponential function whose functional form is

$$RH = a_1 \left(1 - a_2 \exp - \left(\frac{t}{\tau} \right)^\alpha \right) \quad (3.10)$$

The results of the fitting process are shown in Fig. 3.8. The curve and the fit are in excellent agreement. The fitting process is also performed for the hydrogenated and hydrophobically modified cases. For a more detailed analysis see [33] .

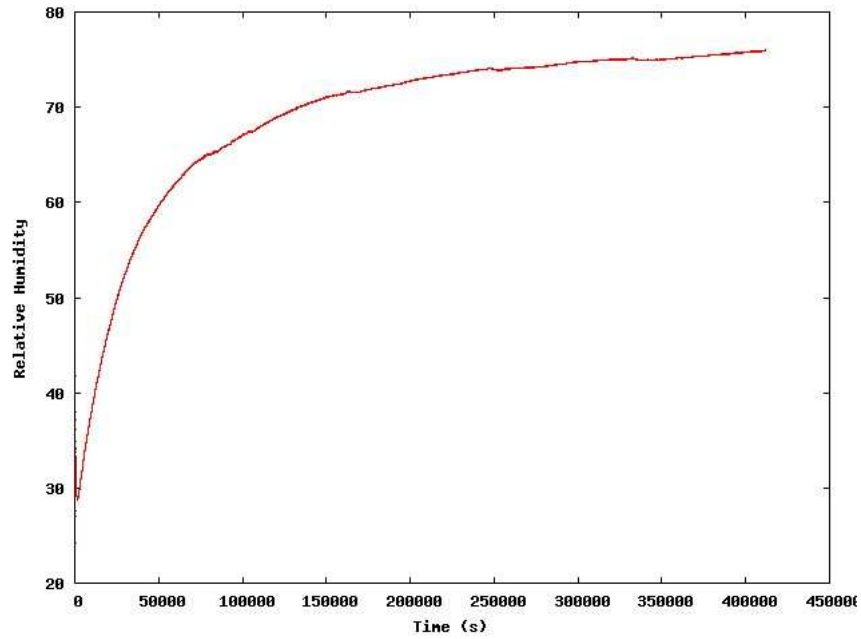


Figure 3.7. Relative Humidity vs. Time of PEG-Si.

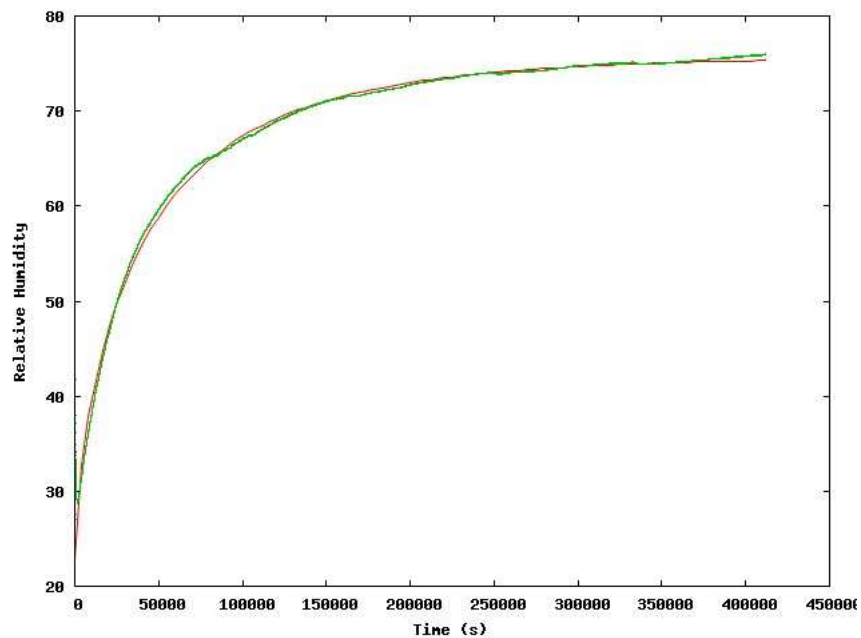


Figure 3.8. Stretched exponential relaxation function fit of the time dependence of Relative Humidity, $RH = a_1(1 - a_2 \exp(-(t/\tau)^\alpha))$ with $a_1 = 75.7259 \pm 0.002161$, $a_2 = 0.699292 \pm 0.0001653$, $\tau = 41041 \pm 15.78$ and $\alpha = 0.686974 \pm 0.0002406$.

4. DETRENDED FLUCTUATION ANALYSIS

In the previous chapter, we applied nonlinear time series analysis to the current time series of the pure, hydrogenated and hydrophobically modified cases. We arrived at the conclusion that for all the cases there is a change of regime for the maximal Lyapunov exponents at some relative humidity value. A second conclusion was that the current instabilities for the latter two cases were decreased and could be tracked by the absolute values of the maximal Lyapunov exponents. To be able to place our conclusions on a firmer ground, we analysed our data with another method, the detrended fluctuation analysis.

Detrended fluctuation analysis was introduced by Peng et al. [35], it is superior to ordinary fluctuation analysis and rescaled range analysis in the sense that, it can be applied to nonstationary data. Basically, DFA is a method for determining the statistical self-affinity of a signal, and is useful for analysing time series that appear to be long-memory processes.

Assuming a time series of the form s_t , the DFA algorithm would read as follows;

- The time series to be analyzed (with N samples) is first integrated digitally as $S_t = \sum_{i=1}^t (s_i - \langle s_i \rangle)$ with $\langle s_i \rangle$ being the the average value.
- The integrated time series is divided into boxes of equal length, n . In each box of length n , a least squares line is fit to the data (representing the trend in that box). The y coordinate of the straight line segments is denoted by $y_n(k)$.
- The integrated time series $y(k)$ is detrended, by subtracting the local trend $y_n(k)$ in each box.
- The root-mean-square fluctuation of this integrated and detrended time series is calculated by

$$F(n) = \sqrt{\frac{1}{N} \sum_{k=1}^N [y(k) - y_n(k)]^2} \quad (4.1)$$

- This computation is repeated over all time scales (box sizes) to characterize the relationship between $F(n)$, the average fluctuation, and the box size, n . Typically, $F(n)$ will increase with box size. A linear relationship on a log-log plot indicates the presence of power law (fractal) scaling. In this case, the fluctuations can be characterized by a scaling exponent, α , the slope of the line relating $\log F(n)$ to $\log n$.

The correlations to which the α values point are listed in Table 4.1. A crossover in the scaling exponent, α , indicates a transition from one type to a different type of underlying correlation, due to a transition in the dynamical properties.

Table 4.1. The correlations implied by the corresponding DFA exponents

$\alpha < \frac{1}{2}$	anti-correlated
$\alpha \simeq \frac{1}{2}$	uncorrelated, white noise
$\alpha > \frac{1}{2}$	correlated
$\alpha \simeq 1$	1/f noise
$\alpha > 1$	non-stationary, random walk like, unbounded
$\alpha \simeq \frac{3}{2}$	Brownian noise

The results of the detrended fluctuation analysis for our data are summarized in Table 4.2. The existence of more than one regime points to the fact that there is a crossover in the scaling exponent.

Table 4.2. DFA exponents

pure PEG-Si	two regimes	1.01, 1.86
hydrophobically modified PEG-Si	one regime	1.93
hydrogenated PEG-Si	two regimes	1.35, 1.84

In summary, the results of the former analysis is as follows; two different regions can be observed in Fig. 4.1 where the slope is discontinuous; this points to changing dynamics of the correlations parallel to the change in the Lyapunov exponents. The discontinuity is distinctly different since the slopes are 1.01 and 1.86. For the hydrophobically modified sample there is one regime with slope 1.93 (Fig. 4.2) pointing to a

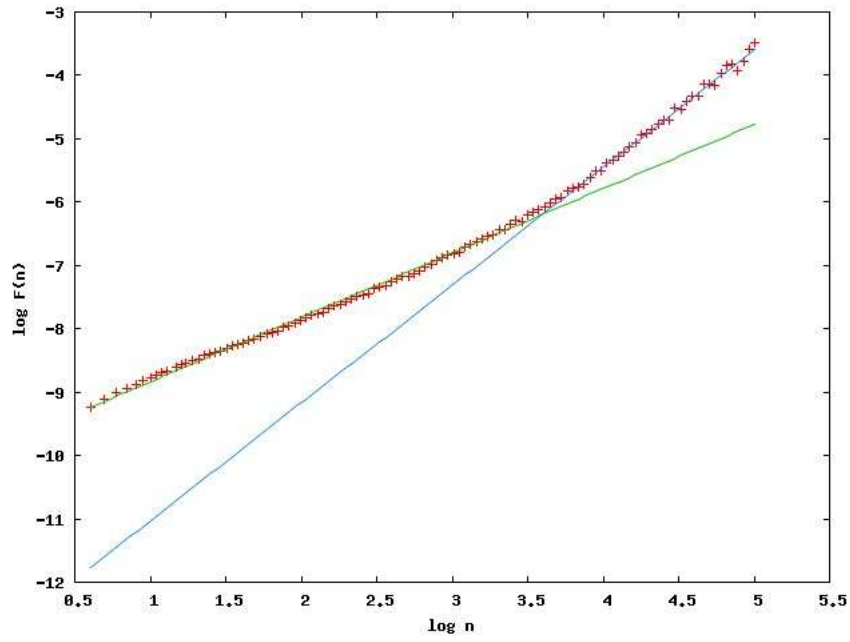


Figure 4.1. Average fluctuation vs. box size for the PEG-Si sample

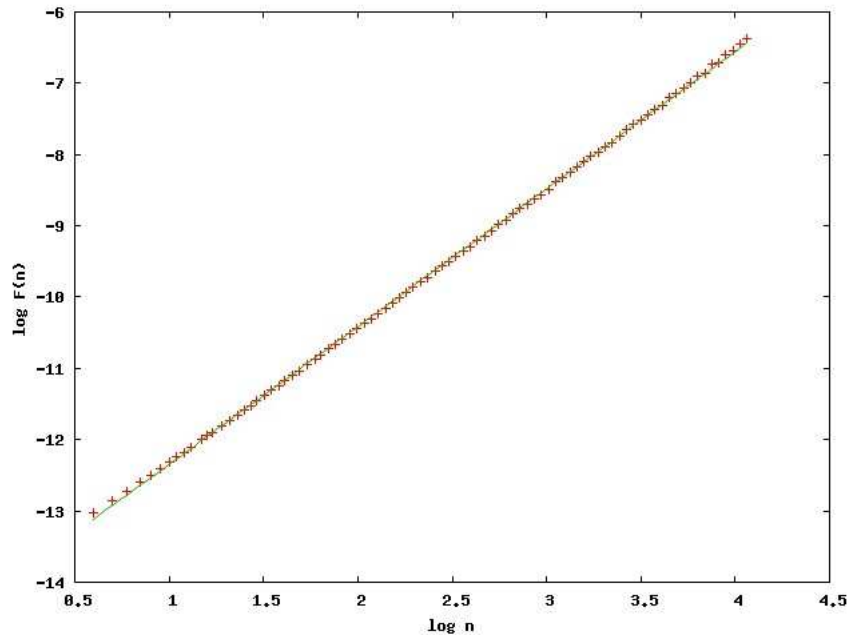


Figure 4.2. Average fluctuation vs. box size for the hydrophobically modified PEG-Si sample

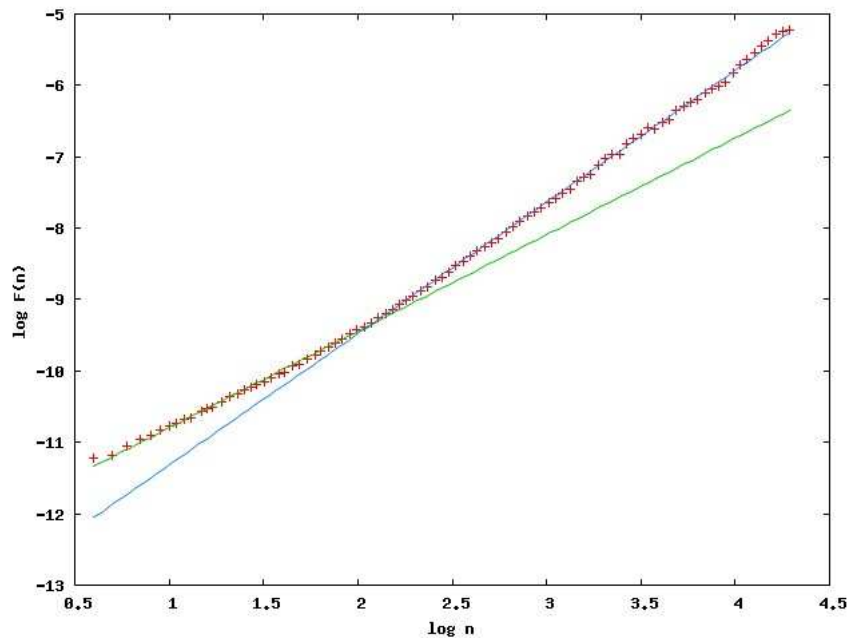


Figure 4.3. Average fluctuation vs. box size for the hydrogenated PEG-Si sample

significant advance in stability (it is noteworthy to mention again that the maximal Lyapunov exponents for the corresponding specimen were smaller in magnitude than those of the other two samples). In the hydrogenated case there are still two different slopes with values 1.35 and 1.84 (Fig. 4.3) indicating an improvement in stability.

5. CONCLUSIONS

The complex structure of polymers (including impurities) implies many degrees of freedom and a multi-fractal structure. The difficulty of obtaining identical results under nearly identical conditions for polymers is well known in the literature [18]. Thus, it becomes necessary to analyze the conductivity of polymers by nonlinear considerations such as maximal Lyapunov exponents and DFA exponents.

The irregular behavior of current through PEG-Si thin films as a function of increasing relative humidity was analyzed using nonlinear time series analysis and detrended fluctuation analysis. Low dimensional chaos with maximal Lyapunov exponents, with an abrupt change of regime around a relative humidity value of 70% is observed. Furthermore, the observed chaotic behavior persists for a wide range of values of the humidity. Hence, the dynamics underlying the current understood in terms of invariants of nonlinear dynamics in the abrupt change of Lyapunov exponents is consistent with the phase transition from semicrystalline state to gel state (for use of Lyapunov exponents as an indicator of phase transitions see [16]). The behavior of the system with different regions has also been confirmed via detrended fluctuation analysis. Even though a general relation between Lyapunov exponent and the DFA exponent has not been reported yet, there are case based studies where analogies between the above mentioned exponents are shown [19]. The change in the scaling exponent in case of phase transition is also reported [20]. This further supports the detection of phase transition in PEG-Si as well as the capability of using nonlinear methods in analyzing behavior of current through PEG-Si thin films. Based on the studies about amorphous materials with irregular behavior, the use of nonlinear methods for analyzing the conductivity mechanisms in such materials seems crucial [6, 7, 21].

The analysis on hydrogenated and hydrophobically modified PEG-Si samples revealed smaller maximal Lyapunov exponents and little or no changes in the DFA exponents, pointing to the fact that their instabilities are milder as compared to the pure PEG-Si samples. In particular, hydrophobically modifying the samples seems to

be a more effective method in reducing the instability as judged from smaller maximal Lyapunov exponents and with a single DFA exponent.

APPENDIX A: Lorenz Equations

The Lorenz system is a popular example of chaotic behavior which deserves to be mentioned. It is a 3-dimensional structure corresponding to the long-term behavior of a chaotic flow, governed by the following equations:

$$\dot{x} = \sigma(y - x) \tag{A.1}$$

$$\dot{y} = \rho x - y - xz \tag{A.2}$$

$$\dot{z} = xy - \beta z \tag{A.3}$$

where σ is called the Prandtl number and ρ is called the Rayleigh number. All σ , β and ρ are greater than zero. Usually $\sigma = 10$, $\beta = 8/3$ and ρ takes different values. With these values of σ and β , the behavior of the system with changing ρ can be summarized as follows:

- With $\rho < 1$, the system has one attracting fixed point, namely $(0, 0, 0)$.
- At $\rho = 1$, the point $(0, 0, 0)$ becomes a repeller, two new fixed points arise, namely, $(\sqrt{\beta(\rho - 1)}, \sqrt{\beta(\rho - 1)}, \rho - 1)$ and $(-\sqrt{\beta(\rho - 1)}, -\sqrt{\beta(\rho - 1)}, \rho - 1)$.
- For $\rho > 24.06$ a strange attractor arises.

For $\sigma = 10$, $\beta = 8/3$ and $\rho = 28$, the strange attractor (Fig. B.1) and the time series of the x component (Fig. B.2) are shown below.

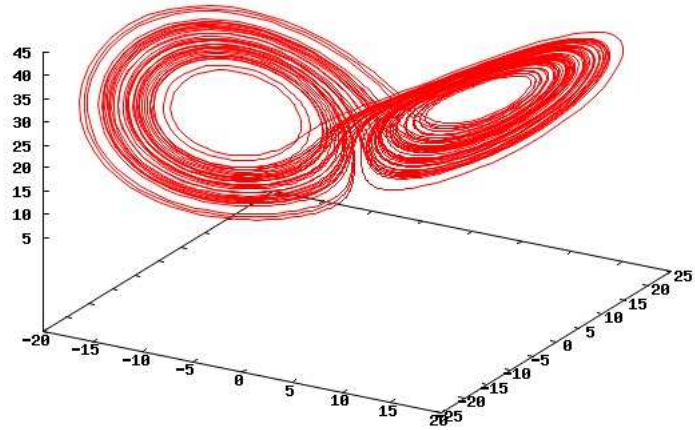


Figure A.1. Lorenz Attractor

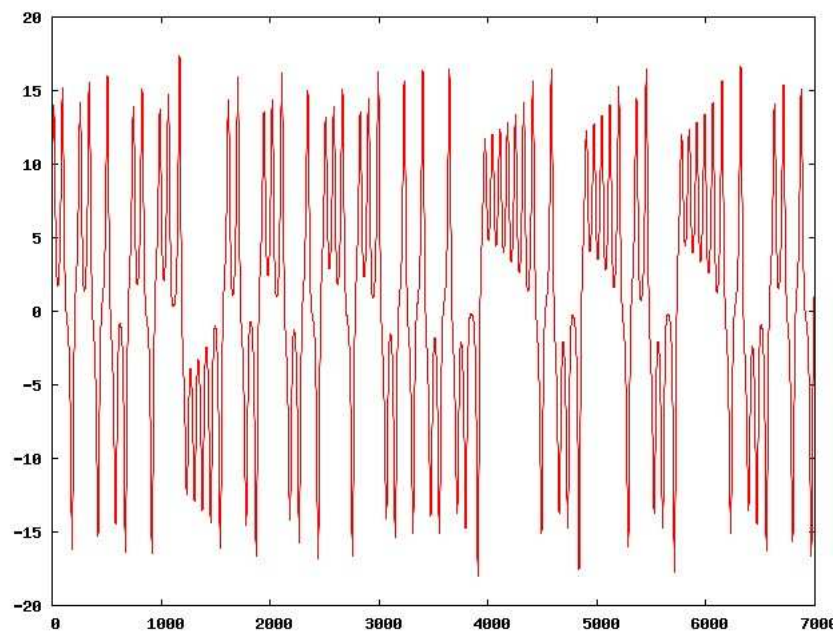


Figure A.2. Time evolution of the first component of the Lorenz Attractor

REFERENCES

1. Abarbanel, H. D. I., R. Brown, J. J. Sidorowich and L. S. Tsimring, "The analysis of observed chaotic data in physical systems", *Rev. Mod. Phys.* 65 1331-1392, 1993
2. Hegger, R., H. G. Kantz and T. Schreiber, *Nonlinear Time Series Analysis*, Cambridge University Press, 1997
3. Sperling, L. H., *Introduction to Physical Polymer Science*, John Wiley & Sons Inc., 2006
4. Erdamar, O., Y. Skarlatos, G. Aktas and M. N. Inci, "Experimental investigation of the humidity induced change in the conduction mechanism of PEG", *Applied Physics A*, Vol. 83, 159-162, 2006
5. Strogatz, S. H., *Nonlinear Dynamics and Chaos*, Perseus Books Publishing, 1994
6. Hacnlyyan, A., Y. Skarlatos, and G. Sahin and G.Akin, "Signals of chaotic behavior in PMMA", *Chaos, Solitons and Fractals* 17 575-583, 2003
7. Hacnlyyan, A., Y. Skarlatos, H. A. Yildirim and G. Sahin, "Simulation of transient current through PMMA thin films based on a random walk model", *Phys. Rev. B* 73 134302, 2006
8. Peng, C. K., S. V. Buldyrev, S. Havlin, M. Simons, H. E. Stanley and A. L. Goldberger, "Mosaic organization of DNA nucleotides", *Phys Rev E* 49, 1685, 1994
9. Peng, C. K., S. Havlin, H. E. Stanley and A. L. Goldberger, "Quantification of scaling exponents and crossover phenomena in nonstationary heartbeat time series", *Chaos*, 5, 82-87, 1995
10. Hu, K., P.Ch. Ivanov, Z. Chen, P.Carpenna and H. E. Stanley, "Effect of trends on detrended fluctuation analysis", *Phys. Rev. E*, 64, 011114, 2001

11. Chen, Z., P. Ch. Ivanov, K. Hu and H. E. Stanley, "Effect of nonstationarities on detrended fluctuation analysis", *Phys. Rev. E*, 65, 041107, 2002
12. Crank, J. and G.S. Park (editors), *Diffusion in Polymers*, Academic Press, London, 1968
13. Chen, W., K. R. Shull, T. Papatheodorou, D. A. Styrkas and J. L. Keddie, "Equilibrium Swelling of Hydrophilic Polyacrylates in Humid Environments", *Macromolecules*, Vol.32, 136-144, 1999
14. Seanor, D. A., *Electrical Properties of Polymers*, Academic Press, New York, 1-58, 1982
15. Nayak, S. K., R. Ramasawamy and C. Chakravarty, "Maximal Lyapunov exponent in small atomic clusters", *Physical Review E*, 51, 3376-3380, 1995
16. Barre, J. and T. Dauxois, "Lyapunov exponents as a dynamical indicator of a phase transition", *Europhysics Letters*, 55, 164-170, 2001
17. Kitano, H. et al., "Fourier transform infrared study on the state of water sorbed to Poly(ethylene glycol) films", *Langmuir*, 17, 1889-1895, 2001
18. Adamec V. and J. H. Calderwood,, "Electrical conduction and polarisation phenomena in polymeric dielectrics at low fields", *J. Phys. D.*, 11, 781-800, 1978
19. Sozanski, M. and J. Zebrowski, "On the application of DFA to the analysis of unimodal maps", *J. Acta Physica Polonica B*, 36, 1803-1821,2005.
20. Zebende, G. F., M. V. S. da Silva, A. C. P. Rosa Jr., A. S. Alves, J. C. O. de Jesus and M. A. More, "Studying long-range correlations in a liquidvapor-phase transition", *Physica A*, 342, 322-328, 2004
21. Hacinliyan, A.,Y. Skarlatos, H. A. Yildirim and G. Sahin, "Characterization of chaoticity in the transient current through PMMA thin films", *Fractals*, 14, 125-

131, 2006

22. Giaretto, V., G. Ruscica and E. Miraldi, "Stretched exponential relaxation analysis of the moisture diffusion in carbon fiber samples", *Modern Physics Letters B*, Vol. 8, pp. 965-975, 1994
23. Bao, L. R., A. F. Yee, Y. Charles and C. Lee, "Moisture absorption and hygrothermal aging in a bismaleimide resin", *Polymer*, Vol.42, 17, 7327-7333, 2001
24. Erdamar, O., Y. Skarlatos, G. Aktas and M. N. Inci, "Experimental investigation of the conduction mechanism of hydrogenated PEG thin films at high relative humidities", *Solid State Ionics*, 177, 3217-3221, 2006
25. Goldberger A. L., L. A. N. Amaral, L. Glass, J. M. Hausdorff, P. Ch. Ivanov, R. G. Mark, J. E. Mietus, G. B. Moody, C. K. Peng and H. E. Stanley. *PhysioBank, PhysioToolkit, and PhysioNet: Components of a New Research Resource for Complex Physiologic Signals*. *Circulation* 101(23):e215-e220 [Circulation Electronic Pages; <http://circ.ahajournals.org/cgi/content/full/101/23/e215>]; 2000 (June 13)
26. Matsaguchi, M., S. Umeda, Y. Sadaoka and Y. Sakai, "Characterization of polymers for a capacitive-type humidity sensor based on water sorption behavior", *Sensors and Actuators B*, 49, 179-185, 1998
27. Aybar, O. Ö. , "Possible chaoticity in condensed matter system", M.S. Thesis, Boğaziçi University, İstanbul, 2008
28. Sahin, G. , "Simulation of transient current through polymethylacrylate thin films based on a charge density wave model", Ph.D. Thesis, Boğaziçi University, İstanbul, 2006
29. Erdamar, Ö. , "Effects of humidity and various gases on the electrical conductivity of polyethylene glycol", Ph.D. Thesis, Boğaziçi University, İstanbul, 2006
30. Şahin, G., "Time series analysis of current in PMMA", M.S. Thesis, Boğaziçi

University, İstanbul, 2001

31. Yıldırım, H. A., “Chaotic structures in conductivity mechanisms”, Ph.D. Thesis, Boğaziçi University, İstanbul, 2005
32. Atak, K., O. O. Aybar, A. Hacınlıyan, G. Şahin and Y. Skarlatos, “Chaoticity analysis of the current through pure, hydrogenated and hydrophobically modified PEG-Si thin films under varying relative humidity”, Central European Journal of Physics, accepted for publication
33. Hacınlıyan, A., Y. Skarlatos, G. Şahin, K. Atak and O. Ö. Aybar, “Possible Stretched Exponential Parametrization for Humidity Absorption in Polymers”, The European Physical Journal E, 28, 369-376, 2009
34. Hegger, R., H. Kantz and T. Schreiber, “Practical implementation of nonlinear time series methods: The TISEAN package”, CHAOS, Vol.94, pp.413-435, 1999
35. Peng, C. K., S. V. Buldyrev, S. Havlin, M. Simons, H. E. Stanley and A. L. Goldberger, “Mosaic organization of DNA nucleotides”, Phys. Rev. E., Vol. 49, pp. 1685-1689, 1994